Unveiling the Inhomogeneous Nature of Strong Field Ionization in Extended Systems

Hyunwook Park, Abraham Camacho Garibay, Zhou Wang, Timothy Gorman, Pierre Agostini, and Louis F. DiMauro

Phys. Rev. Lett. **129**, 203202 — Published 9 November 2022

DOI: 10.1103/PhysRevLett.129.203202

Unveiling the inhomogeneous nature of strong field ionization in extended systems

Hyunwook Park,[1] Abraham Camacho Garibay,[1] Zhou Wang,[1]
Timothy Gorman,[1] Pierre Agostini,[1] and Louis F. DiMauro[1,*]

[1] *Department of Physics, The Ohio State University, Columbus, OH, USA*

(Dated: September 16, 2022)

Intense light-induced fragmentation of spherical clusters produces highly energetic ions with characteristic spatial distributions. By subjecting argon clusters to a wavelength tunable laser, we show that ion emission energy and anisotropy can be controlled through the wavelength - isotropic and energetic for shorter wavelengths and increasingly anisotropic at longer wavelengths. The anisotropic part of the energy spectrum, consisting of multiply charged high energy ions, is considerably more prominent at longer wavelengths. Classical molecular dynamics simulations reveal that cluster ionization occurs inhomogeneously producing a column-like charge distribution along the laser polarization direction. This previously unknown distribution results from the dipole response of the neutral cluster which creates an enhanced field at the surface, preferentially triggering ionization at the poles. The subsequently formed nanoplasma provides an additional wavelength-dependent ionization mechanism through collisional ionization, efficiently homogenizing the system only at short wavelengths close to resonance. Our results open the door to study polarization induced effects in nanostructures and complex molecules and provide a missing piece in our understanding of anisotropic ion emission.

When subjected to intense laser pulses rare gas nanoclusters efficiently absorb energy in quantities far exceeding those observed in the case of gases and solids, emitting photons with wavelengths reaching the X-ray regime, fast energetic electrons, and highly charged ions. As the laser field ionizes a cluster, the released electrons can be field-driven back allowing for an energetic recollision, giving rise to further ionization, backscattered electrons with higher energies, and high harmonic generation (HHG). For electron emission and HHG, it is clear that linearly polarized pulses induce inherently anisotropic dynamics due to the one-dimensional driving field. Somewhat unexpectedly, ionic emission is also observed to proceed anisotropically [1–9], despite the fact that the laser frequency is too fast and the pulse too short to appreciably accelerate these heavy particles. Instead, the constituent atoms can be regarded as fixed in space during the timescale of the pulse duration, acquiring instead their kinetic energy from repulsive electrostatic and hydrodynamic forces acting upon them after the pulse is gone. The mechanisms dictating the directionality of ion emission is central to understanding laser interactions in extended systems and can potentially provide new ways to control and induce dynamics in more complex systems by using more complicated sculpted laser fields.

Depending on the interaction parameters, cluster fragmentation predominantly follows two distinct mechanisms, namely hydrodynamic expansion (HE) and Coulomb explosion (CE). Hydrodynamic expansion is prevalent when laser-cluster interaction follows that of a nanoplasma [10–13] in which inner ionized electrons in a quasi-neutral cluster absorb energy via inverse Bremsstrahlung (IBS) leading to disintegration through the emerging electronic pressure. Coulomb explosion, in contrast, arises from the buildup of a net positive charge in the cluster, which disintegrates through the resulting electrostatic repulsion. This CE mechanisms dominates in small clusters or when photon energies are larger than the atomic ionization potential [14–16]. Experimental results have shown [17] that under many scenarios both mechanisms occur simultaneously, CE being responsible for the emission of the most energetic ions produced in the outermost layers of the cluster, while HE takes place at the quasi-neutral core. As both HE and CE mechanisms predict isotropic ionic emission for homogeneous spherical systems, several interpretations and mechanisms have been proposed to explain the observed anisotropy. In an early effort, Ishikawa et al. [18] suggested that a sub-cycle ultrafast recombination induced by the resonantly moving electron cloud transiently modifies the ionic charge states producing an enhanced field acceleration. Expanding this idea by adding the effect of the Coulomb field and further electron removal at the poles, the "charge flipping" mechanism was introduced [1–3, 6–8]. In this mechanism a net sub-cycle laser field acceleration is further enhanced by higher ion charge states, closely relating anisotropy with energy absorption. In an alternative proposal [19–21], the Coulomb field takes a key role in the form of Polarization Enhanced Ionization (PEI) where electron depletion occurs at the poles every half cycle creating highly charged ions. A sub-cycle screening mechanism by the electron cloud was put forward by Breizman and others [22, 23] to explain anisotropy in Hydrogen clusters without relying on high charge states. Another approach [4, 24, 25] relies on impact ionization by returning outer ionized electrons, characteristic of strong field phenomena, which can potentially deposit vast amounts of energy at the cluster poles in a process denominated vacuum heating. Despite enormous effort, a comprehensive picture has not emerged,

as several explanations are not mutually exclusive and can even occur simultaneously due to the complex dynamics of extended systems. Experimental evaluation of the limits, merits and validity of each mechanism is still necessary. So far, most experiments have been limited to driver wavelengths of either 0.8 or 1 μm. Thus, the experimental observables are investigated by varying the cluster size and composition, laser intensity, and pulse duration, parameters for which most processes predict similar qualitative trends, thus being insufficient to challenge different theoretical models. However, the largely unexplored effect of the driver wavelength, particularly at longer wavelengths ($> 1\mu$m), remains a missing test to explore and potentially unveil hidden aspects of the interaction of complex systems with strong laser fields.

In this Letter, for the first time, an intense tunable femtosecond near infrared (NIR) laser source, ranging from 0.8 to 2.0 μm, is used to explore the continuous and smooth evolution of the cluster ionization, relaxation, and anisotropy, providing test for previous models and new insight into the anisotropic ionic emission. As wavelength is increased (at fixed intensity), emission evolves from an isotropic and energetic hydrodynamic expansion of highly charged ions to an increasingly anisotropic Coulomb explosion with lower ionic energies and charge states. Thus, anisotropy is enhanced from interaction conditions favoring lower energy absorption and fewer ionized electrons, an observation at odds with most proposed mechanisms. As previous theoretical efforts do not provide a satisfactory explanation for our observations, we use classical molecular dynamics (MD) simulations to gain a deeper understanding. Our MD results reveal a novel mechanism for anisotropic emission, closely linked to strong field ionization in extended systems and capable of explaining our observations as well as some previously reported results.

In our experiment argon clusters are produced in an Even-Lavie LAMID ultrasonic jet pulsed valve with estimated [26, 27] average size of 5 nm radius (150 μm-hole trumpet nozzle, 16 bar stagnation pressure). A skimmer collimates the free jet into a molecular beam that propagates into a differentially pumped vacuum chamber equipped with a time-of-flight electron/ion analyzer. As the analyzer position is fixed, the laser polarization is rotated to measure ion emission different directions. Near-infrared pulses are focused by a 100 mm focal length lens, crossing the cluster beam in the spectrometer. The wavelength is varied from 1.2 to 2.0 μm using an optical parametric amplifier (OPA) pumped by a 40 fs, 0.8 μm Ti:Sapphire laser. Laser intensity is calibrated by observing the classical 2Up feature (Up is the ponderomotive energy) in the photoelectron energy distribution of neon and argon atomic gases [28]. Pulse duration in the second moment was extracted using frequency-resolved optical gating (FROG) and measured concurrently with the ion experiments at all wavelengths. Note that the second moment better represents a complex pulse shape [29]. Pulse duration is fixed to 60 fs (FWHM) using a 10 mm thick SF11 glass windows at 1.5 μm and a 6 mm ZnS one at 2.0 μm. The emitted ions travel to a microchannel plate detector under field-free conditions. For charge-state sorting, potential barriers are applied downstream of the field-free interaction region.

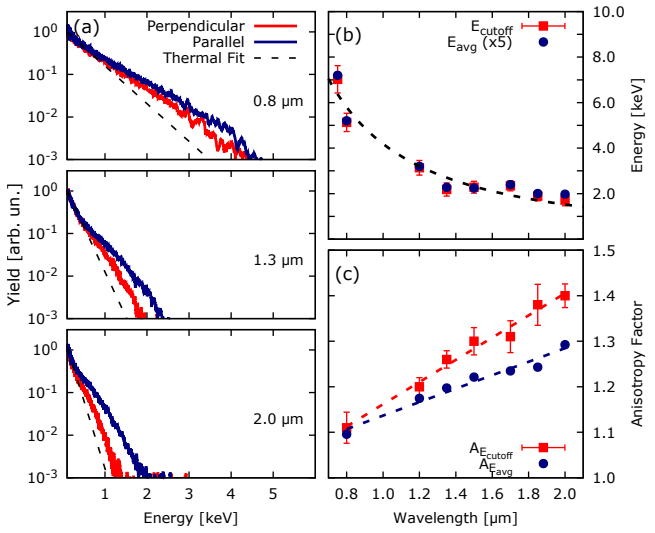

FIG. 1. (a) Ion energy spectra for constant intensity at 0.8, 1.3, and 2.0 μm in parallel (blue) and perpendicular (red) direction with respect to the laser polarization. Dashed lines show an exponential decay fit. (b) Cutoff (red) and mean (blue, 5x) energy with respect to wavelength. A power law fit of energy cutoff yields $E_{cutoff} \propto \lambda^{-1.4\pm0.1}$ (dashed). (c) Anisotropy factor $A_E = E_{\parallel}/E_{\perp}$ calculated for mean (blue) and cutoff (red) energies, along with the corresponding linear fit.

Figure 1(a) shows kinetic energy distributions of ions emitted along parallel (blue) and perpendicular (red) directions with respect to the laser linear polarization axis for 500 TW/cm^2, 60 fs pulses at 0.8, 1.3 and 2.0 μm wavelengths. Ionic emission is nearly isotropic with high energies at 0.8 μm but the cutoff and average energies rapidly diminish with increasing wavelength, while directionality clearly emerges. Ionic energies and anisotropy factors are quantified in Figs. 1(b,c), respectively, at different wavelengths. An anisotropy factor A_E is defined here as the ratio of the ion energy emitted parallel and perpendicular to the polarization axis, $A_E = {}^{E_\parallel}/_{E_\perp}$. The reduction in ionic energies is consistent with the nanoplasma model [11] since heating rates decreases as the laser is red detuned from the plasma frequency, i.e., 0.2 μm. However, the simultaneous increase in anisotropy at longer wavelengths is in direct conflict with the predictions of most proposed mechanisms correlating the anisotropy directly to the energy absorption. Moreover, it has been previously demonstrated in clusters that longer wavelengths give rise to high-energy electron emission [30] consis-

tent with single atom behavior in strong fields, excluding plasma effects.

Closer inspection of the ion distributions reveals that for all wavelengths the low energy portion is well described by a decaying exponential function, i.e., a thermal distribution describing hydrodynamic expansion (HE). Even so, this fit systematically underestimates yields at the higher end of the distribution and the discrepancy grows with increasing wavelength, becoming a prominent knee-shaped structure. We attribute these non-thermal features in the ion energy distribution to Coulomb explosion (CE) of surface ions, as previously reported in argon and xenon cluster experiments [17] and numerically for high-temperature plasma expansions [31, 32]. In addition, theoretical studies of clusters under XFEL pulses [16] demonstrated that ion expansion can be controlled through wavelength, transitioning from pure CE for soft X-rays to full HE for VUV pulses. However, our NIR results point to a similar wavelength-dependent transition in ion expansion with the caveat of a reversed trend, where CE of low energy ions becomes more dominant at longer wavelengths. Additional evidence of this transition is provided by the anisotropy factor A_E in Figure 1(c), extracted using either the ion cutoff or average energies. If the relative importance of CE and HE were constant for different wavelengths, A_{E_c} and $A_{\langle E\rangle}$ would evolve with the same slope or have identical values if one mechanism dominates the expansion. Instead, we observe a similar trend with different slopes, suggesting dissimilar expansions for different wavelengths. It can be inferred that A_{E_c}, calculated from surface ejected ions, captures an inhomogeneity in the CE of the surface, while $A_{\langle E\rangle}$ being a measure of the overall spectra carry information of the HE to CE transition.

Charge-sorted spectra obtained at 1.8 µm provides additional insight (see supplement figure S1) as low-charge state ions ($q \leq 2$) are emitted isotropically closely following an exponential decay, whereas energetic high-charge ions ($q \geq 5$) display clear directional emission along the laser polarization. Furthermore, high-charge ions display non-thermal features in both directions, resembling a log-normal distribution with small yields at low energies, similar to size distributions of supersonic cluster jets [26, 27]. From geometric arguments, ions located close to the cluster core acquire small kinetic energies due to the system symmetry, independently of their charge state. The absence of high-charged ions at low energies, evidenced by the roll off and large noise fluctuations in the distribution low energy portion, suggests that these states are emitted from the outermost layers of the cluster. Complementing this idea, low-energy ions comprising the thermal portion of the spectra are therefore produced inside a quasi-neutral plasma confined at the core. As the thermal ion yield is reduced with increasing wavelength, it follows that the number of inner-ionized electrons also decreases, producing a colder, more compact plasma. These observations conflict with mechanisms relying on large numbers of inner-ionized electrons to explain anisotropy, such as PEI and Sub-cycle Screening [19–23].

The observed wavelength dependence of anisotropy is only qualitatively consistent with the vacuum heating mechanism [4, 24, 25], which surmises that field driven electrons deposit additional energy at the cluster poles. However, the returning electron energies scale according to λ^2 implying either larger ionic energies or deeper penetration into the cluster, in contradiction with our observations. In fact, extrapolating the observed trends to the longer wavelength limit leads to the perplexing scenario of a system with no plasma electrons displaying the largest emission anisotropy. This corresponds to a pure Coulomb explosion of a spherical system with a laser induced inhomogeneous charge distribution, for which a new paradigm seems necessary.

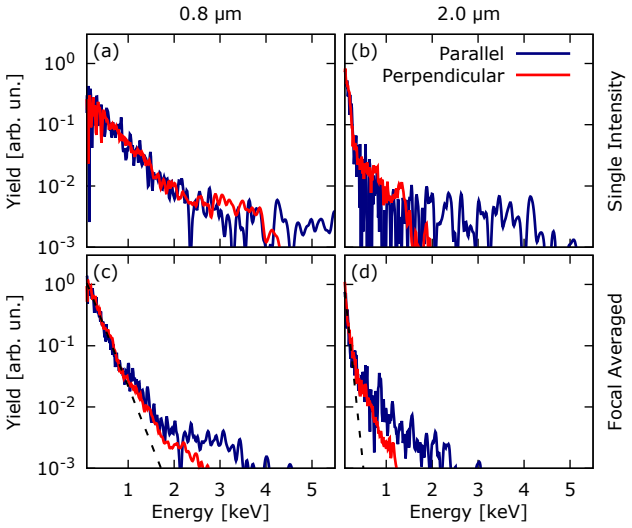

FIG. 2. Molecular Dynamics simulated ion energy spectra in parallel (blue) and perpendicular (red) directions with respect to polarization direction for 0.8 and 2.0 µm wavelengths. (a, b) Single intensity spectra for clusters of radius R = 3.2 nm, containing N = 2725 atoms. (c, d) Focal averaged spectra for a Gaussian intensity profile with peak intensity of 500 TW/cm^2. Dashed lines provide an exponential decay fit in good agreement at low energies, signature of hydrodynamic expansion.

Clearly, a more complete interpretation requires evaluating the effect of laser driven returning electrons and the ionization dynamics. To that end, we performed a detailed theoretical investigation through microscopic three-dimensional classical molecular dynamics (MD) simulations in clusters of 3.2 nm radius, subjected to pulses of varying wavelength. In our simulations, all particles are classically propagated following Newton's equations of motion incorporating all particle-particle interactions [14, 15], implementing atomic ionization via

soft-core potentials for both field and electron impact ionization, and electron-electron interactions through the corresponding Coulomb potential. Initial conditions are chosen such that singly charged ions are located inside a sphere of radius R_0 with icosahedral structure, and for each one a single electron is positioned near their corresponding potential minimum. Once the laser field interacts with the system and electrons gain enough energy to leave the vicinity of their parent ion (given by their van der Waals radius), the ion charge increases by one unit and an additional electron is incorporated to the calculation at the bottom of the updated potential. Propagation times of 1 ps after the peak of the pulse ensure energetic and statistical convergence, for an ensemble of randomly oriented clusters and slightly different initial positions. Simulations were also extended to the EUV spectral domain by including appropriate single-photon ionization cross-sections for photon energies larger than the ionization potential. Such simulation scheme has successfully been used to study high-energy electron emission in clusters at long wavelengths [30].

Figure 2 shows simulated ion spectra for single size clusters of 3.2 nm radius subjected to 60 fs Gaussian pulses at 0.8 and 2.0 µm. Single intensity results for 500 TW/cm^2 (Fig.2a, b) reveal that NIR pulses create considerably more energetic ions along the polarization direction for both wavelengths. Nonetheless we observe two key differences at longer wavelengths, (1) larger fraction of ions ejected anisotropically and (2) a higher anisotropy factor A_E. However, experimental results are measured over the laser intensity profile of a statistical ensemble of clusters with different sizes. While we restrict our discussion to single size simulations for clarity, we also incorporated focal averaging effects through a weighted sum of single intensity calculations to reflect the laser profile (Fig. 2c, d). Results from both single intensity and focal averaged spectra reproduce the main experimental observations: reduced ion energy at longer wavelength, isotropic HE signature with exponential decay distributions at low energies and knee-shaped structures at high energies associated with CE extending even further along the laser polarization direction. While anisotropy is observed for both wavelengths, a larger ionic fraction belongs to the CE knee feature at 2.0 µm despite the lower energies, a difference further amplified by focal averaging.

Our calculations are summarized in Figure 3, showing an efficient energy absorption at shorter wavelengths (3a), i.e. near the plasma frequency. However, absorption does not continue indefinitely, as reflected by the sudden drop in ion energy for wavelengths below 0.2 µm. In the VUV regime multiphoton processes are rapidly outpaced by the dominating single photon ionization, and such high-frequency fields only weakly drive inner-ionized electrons, vastly reducing collisional events rendering inverse Bremsstrahlung an inefficient heating mechanism. The anisotropy factors (3b) derived from MD display

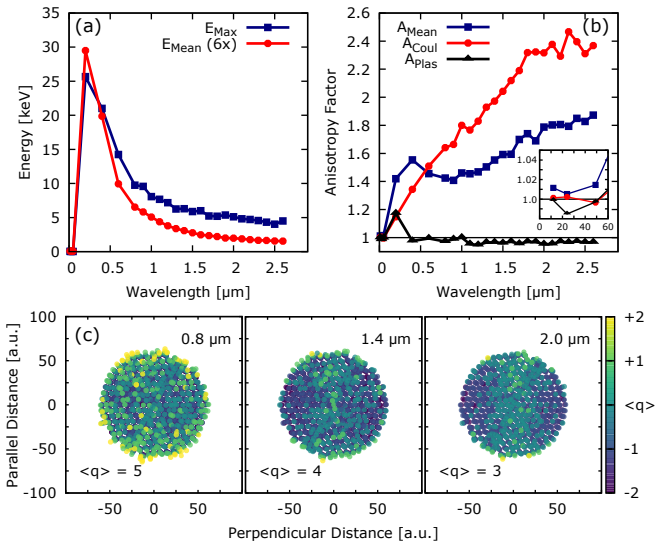

FIG. 3. (a) Maximum (blue) and average (red) ionic energy with respect to wavelength. Energy absorption is most efficient close to the plasma frequency (200 nm). (b) Anisotropy factors calculated using the total (blue), Coulomb (red) and plasma (black) fractions of the ion spectra (see text). Inset provides a better visualization for the quantities in the EUV range (please notice the inset units on the x axis are nanometers). Calculations for both figures range from the mid-infrared (2.6 µm) down to the EUV (12 nm). (c) 2D projection of Ar clusters (R = 3.2 nm, N = 2725 atoms), displaying the ionic charge states when subjected to an intense laser pulse ($\tau = 60$ fs) at the pulse peak for different wavelengths. Charge distribution is nearly isotropic for short wavelengths, and highly anisotropic for long ones as charging has not yet reached the whole system.

different trends when A_E is computed using the entire spectrum or restricted to the CE fraction. Anisotropy from the Coulomb portion (A_{E_C}) increases linearly from isotropic emission at the high-frequency limit until reaching a saturation value as the wavelength approaches the few-cycle regime. Additionally, the computed $A_{\langle E \rangle}$ using the average energies features an additional enhancement close to the typical plasma frequency of about 0.2 µm. This feature is attributed solely to the plasma portion of the spectra (A_{E_P}), therefore restricting plasmonic-based mechanisms [33] as a feasible source for emission anisotropy to a narrow frequency window. This spectral region, interesting in its own right, falls outside the scope of the present work.

Additional insight is gained by cross-referencing the time and position of ionization events and electron-ion collisions, demonstrating that vacuum heating is negligible, in particular at longer wavelengths, i.e., only 5% of ionized electrons at 2 µm are collisional. We find that, contrary to the common assumption of homogeneous expansion, at early stages of laser-cluster interaction the charge distribution resembles a column along the polarization axis. Unlike atomic argon, the near solid den-

sity of clusters implies that interatomic dipole interactions (and by extension, the cluster polarizability) can no longer be neglected. The dipole field induced by NIR pulses produce an antiparallel homogeneous field inside the cluster body while an angular dependent field acts on its surface according to $\mathbf{E_d}(\mathbf{R}) = \frac{\gamma}{r_{VW}^3}(3\mathbf{n}(\mathbf{n}\cdot\mathbf{E}_\omega) - \mathbf{E}_\omega)$, where γ is the atomic polarizability, $r_{\rm vw}$ the Van der Waals atomic radius, $\mathbf{E}_\omega$ the incident laser field, and $\mathbf{R}$ a vector of length equal to the cluster radius R along the radial unit vector $\mathbf{n}$ [34]. The dipole field is size independent and proportional to the laser field, adding to the total field with a maximum value at the cluster pole in the direction of the laser according to $\mathbf{E}_\parallel = (1 + 2\gamma/r_{\rm vw}^3)\mathbf{E}_\omega$ while the bulk experiences a reduced field $\mathbf{E_{in}} = (1 - \gamma/r_{\rm vw}^3)\mathbf{E}_\omega$. Our numerical implementation increases the total field at the poles by $\sim 40\%$ similar to what can be expected experimentally, greatly impacting the highly nonlinear ionization rates and making the cluster poles preferential sites for ionization. Indeed, we observe in our calculations that ionization invariably starts at the poles for all wavelengths (see Supplemental material). Previous works in Xe doped helium nanodroplets [35–37] have shown that preferential sites for ionization produce cigar-shaped plasmas, and here we demonstrate that such inhomogeneous charge distributions are the rule rather than the exception in extended systems. It should be emphasized that this dipole field is not a nanoplasma effect, it is a collective response of bound electrons in the system.

The cluster dipole response provides a natural explanation for emission anisotropy, inducing the formation of inhomogeneous charge distributions. However, it does not explain the observed wavelength dependence since dipole fields are frequency independent. While ionization rates exhibit some dependence the laser frequency according to PPT rates [38], and non-adiabatic effects can excite the system prior to ionization [39], these effects are expected to be negligible. Instead, dependence is indirectly introduced through inverse Bremsstrahlung from inner-ionized plasma electrons since the collision frequency (and therefore heating and thermal ionization rates) decreases with wavelength. Thus, shorter wavelengths (1) produce larger amounts of plasma electrons and (2) ions with higher charge states thus resulting in an enhanced laser energy absorption. Hotter plasma electrons rapidly homogenize the local charge distribution inside the cluster (see Supplemental material) either through thermal ionization or by screening highly charged ions. Figure 3 (c) shows a transversal slice with the ion positions and charge states at the peak of the pulse for different wavelengths, obtained from the MD simulations. The color scale is centered around the (integer) average ion charge to aid visualization. A column-like distribution is appreciated at 2.0 μm (laser polarization along the vertical axis) almost entirely containing higher charge ions, while the equator is significantly less ionized. This striking inhomogeneity is less apparent at 1.4 μm but the distribution is still clearly concentrated along the axis with lower charges at the equator, while finally at 0.8 μm charge appears to be almost radially symmetric. In consequence, as the pulse ends and the cluster disintegrates, the outermost ions Coulomb explode acquiring energies proportional to their charge states, thus producing the observed anisotropy. Plasma electrons in turn remain close to the potential minimum at the cluster center, creating a quasi-neutral core that hydrodynamically expands.

In summary, we presented a comprehensive experimental and theoretical study of the wavelength dependent ion expansion, energy and anisotropy resulting in new insight of the laser-cluster dynamics, specifically the prominent role of the dipole response. The wavelength dependence provides a new detailed view of the ionization process consistent with observations in experiment and theory while eliminating previously proposed mechanisms such as PEI, "charge flipping", or vacuum heating. We have identified that, due to the polarizability of the constituting particles, strong field ionization in extended systems inherently gives rise to inhomogeneous charge distributions favoring anisotropic Coulomb explosions, while subsequent heating mask the effect by homogenizing the observable at shorter wavelengths. We hope our results bring attention to polarizability induced effects that, as we have demonstrated, can significantly influence the ionization dynamics of extended systems subjected to NIR pulses and could potentially produce interesting new phenomena.

* dimauro.6@osu.edu

[1] V. Kumarappan, M. Krishnamurthy, and D. Mathur, *Asymmetric High-Energy Ion Emission from Argon Clusters in Intense Laser Fields.* Phys Rev Lett. **87**, (2001)

[2] V. Kumarappan, M. Krishnamurthy and D. Mathur, *Asymmetric emission of high-energy electrons in the two-dimensional hydrodynamic expansion of large xenon clusters irradiated by intense laser fields.* Phys. Rev. A **67**, 043204 (2003).

[3] M. Krishnamurthy, D. Mathur, and V. Kumarappan, *Anisotropic "charge-flipping" acceleration of highly charged ions from clusters in strong optical fields.* Phys. Rev. A **69**, (2004).

[4] D. R. Symes, M. Hohenberger, A. Henig and T. Ditmire, *Anisotropic Explosions of Hydrogen Clusters under Intense Femtosecond Laser Irradiation.* Phys. Rev. Lett. **98**, 123401 (2007).

[5] E. Skopalová, Y. C. El-Taha, A. Zaïr, M. Hohenberger, E. Springate, J. W. G. Tisch, et al., *Pulse-Length Dependence of the Anisotropy of Laser-Driven Cluster Explosions: Transition to the Impulsive Regime for Pulses Approaching the Few-Cycle Limit.* Phys Rev Lett. **104**, (2010).

[6] D. Mathur, and F. A. Rajgara, *Communication: Ioniza-*

tion and Coulomb explosion of xenon clusters by intense, few-cycle laser pulses. The Journal of Chemical Physics **133**, (2010).

[7] D. Mathur, F. A. Rajgara, A. R. Holkundkar, N. K. Gupta, *Strong-field ionization and Coulomb explosion of argon clusters by few-cycle laser pulses.* Phys Rev A. **82**, (2010).

[8] D. Mathur and F. A. Rajgara, *Dynamics of Atomic Clusters in Intense Optical Fields of Ultrashort Duration.* J. Chem. Sci., **124** 75 (2012).

[9] G. Mishra, N. K. Gupta, *Molecular dynamic studies on anisotropic explosion of laser irradiated Xe cluster.* Physics of Plasmas. **19**, (2012).

[10] T. Ditmire, T. Donnelly, A. M. Rubenchik, R. W. Falcone, M. D. Perry, *Interaction of intense laser pulses with atomic clusters.* Phys Rev A. **53** (1996).

[11] T. Ditmire, *Simulation of exploding clusters ionized by high-intensity femtosecond laser pulses.* Phys Rev A. **57** (1998).

[12] J. W. G. Tisch, *Atoms, Solids, and Plasmas in Super-Intense Laser Fields.* Edited by D. Batani, C. J. Joachain, S. Martellucci, and A. N. Chester (Springer US, Boston, MA, 2001).

[13] J. H. Posthumus, *Molecules and Clusters in Intense Laser Fields.* (Cambridge University Press, Cambridge, England, 2001).

[14] U. Saalmann, C. Siedschlag and J. M. Rost, *Mechanisms of cluster ionization in strong laser pulses.*. J. Phys. B: At. Mol. Opt. Phys. **39**, R39–R77 (2006).

[15] T. Fennel, K.-H. Meiwes-Broer, J. Tiggesbäumker, P.-G. Reinhard, P. M. Dinh, and E. Suraud, *Laser-Driven Nonlinear Cluster Dynamics.* Rev. Mod. Phys. **82** 1793 (2010).

[16] M. Arbeiter and T. Fennel, *Rare-Gas Clusters in Intense VUV, XUV and Soft x-Ray Pulses: Signatures of the Transition from Nanoplasma-Driven Cluster Expansion to Coulomb Explosion in Ion and Electron Spectra.* New J. Phys. **13** 053022 (2011).

[17] M. Lezius, S. Dobosz, D. Normand, and M. Schmidt, *Explosion Dynamics of Rare Gas Clusters in Strong Laser Fields.* Phys. Rev. Lett. **80** 261 (1998).

[18] K. Ishikawa and T. Blenski, *Explosion Dynamics of Rare-Gas Clusters in an Intense Laser Field.* Phys. Rev. A **62** 063204 (2000).

[19] C. Jungreuthmayer, M. Geissler, J. Zanghellini, and T. Brabec, *Microscopic Analysis of Large-Cluster Explosion in Intense Laser Fields.* Phys. Rev. Lett. **92** 133401 (2004).

[20] C. Deiss, N. Rohringer, and J. Burgdörfer, *Interaction of Ultra-Short Laser Pulses with Clusters: Short-Time Dynamics of a Nano-Plasma.* AIP Conference Proceedings, Vol. 876 (AIP, National Park Kopaonik (Serbia), 2006), pp. 143–153.

[21] C. Prigent, C. Deiss, E. Lamour, J.-P. Rozet, D. Vernhet, and J. Burgdörfer, *Effect of Pulse Duration on the X-Ray Emission from Ar Clusters in Intense Laser Fields.* Phys. Rev. A **78** 053201 (2008).

[22] B. N. Breizman, A. V. Arefiev, and M. V. Fomyts'kyi, *Nonlinear Physics of Laser-Irradiated Microclusters.*, Physics of Plasmas **12**, 056706 (2005).

[23] C. Peltz, C. Varin, T. Brabec, and T. Fennel, *Time-Resolved X-Ray Imaging of Anisotropic Nanoplasma Expansion.*, Phys. Rev. Lett. **113**, 133401 (2014).

[24] A. V. Getz and V. P. Krainov, *Vacuum Heating of Large Atomic Clusters by a Superintense Femtosecond Laser Pulse.*, J. Exp. Theor. Phys. **101**, 80 (2005).

[25] M. Hirokane, S. Shimizu, M. Hashida, S. Okada, S. Okihara, F. Sato, T. Iida, and S. Sakabe, *Energy Distributions of Ions Emitted from Argon Clusters Coulomb-Exploded by Intense Femtosecond Laser Pulses.*, Phys. Rev. A **69**, 063201 (2004).

[26] O.F. Hagena, *Condensation in free jets: Comparison of rare gases and metals.*, Z. Phys. D - Atoms, Molecules and Clusters **4**, 291–299 (1987).

[27] O.F. Hagena, *Cluster ion sources (invited).*, Review of Scientific Instruments **63**, 2374–2379 (1992).

[28] P. Colosimo, G. Doumy, C.I. Blaga, J. Wheeler, C. Hauri, F. Catoire, J. Tate, R. Chirla, A.M. March, G.G. Paulus, H.G. Muller, P. Agostini, and L.F. DiMauro, *Scaling strong-field interactions towards the classical limit.*, Nature Phys **4**, 386–389 (2008).

[29] JC Diels and W. Rudolph, *Ultrashort laser pulse phenomena: Fundamentals, Techniques and Applications on a Femtosecond Time Scale, second edition.* (Academic Press, London, 2006) p.15.

[30] Z. Wang, A. Camacho Garibay. H. Park, U. Saalmann, P. Agostini, J. M. Rost, and L.F. DiMauro, *Universal High-Energy photoelectron emission from nanoclusters beyond the atomic limit.*, Phys. Rev. Lett. **124**, 173201 (2020).

[31] F. Peano, G. Coppa, F. Peinetti, R. Mulas, and L. O. Silva, *Ergodic Model for the Expansion of Spherical Nanoplasmas.*, Phys. Rev. E **75**, 066403 (2007).

[32] A. Beck and F. Pantellini, *Spherical Expansion of a Collisionless Plasma into Vacuum: Self-Similar Solution and Ab Initio Simulations.* Plasma Phys. Control. Fusion **51**, 015004 (2009).

[33] J. Passig, R. Irsig, N. X. Truong, Th. Fennel, J. Tiggesbäumker, and K. H. Meiwes-Broer, *Nanoplasmonic electron acceleration in silver clusters studied by angular-resolved electron spectroscopy.* New J. Phys. **14**, 085020 (2012).

[34] J. D. Jackson, *Classical electrodynamics.* 3rd edition (Wiley, New York, 1999).

[35] A. Mikaberidze, U. Saalmann and J. M. Rost, *Energy absorption of xenon clusters in helium nanodroplets under strong laser pulses.* Phys. Rev. A **77**, 041201(R) (2008).

[36] A. Mikaberidze, U. Saalmann and J. M. Rost, *Laser-Driven Nanoplasmas in Doped Helium Droplets: Local Ignition and Anisotropic Growth.* Phys. Rev. Lett. **102**, 128102 (2009).

[37] S. R. Krishnan, L. Fechner, M. Kremer, V. Sharma, B. Fischer, N. Camus et al., *Dopant-Induced Ignition of Helium Nanodroplets in Intense Few-Cycle Laser Pulses.* Phys. Rev. Lett. **107**, 173402 (2011).

[38] A. M. Perelomov, V. S. Popov, and M. V. Terent'Ev, *Ionization of atoms in an alternating electric field.* Soviet Physics JETP, **23-5** (1966).

[39] E. Saydanzad, J. Li, and U. Thumm, *Characterization of induced nanoplasmonic fields in time-resolved photoemission: A classical trajectory approach applied to gold nanospheres.* Phys. Rev. A **95**, 053406 (2017).